Hybrid Filter Banks with Fractional Delays: Minimax Design and Application to Multichannel Sampling

Ha T. Nguyen and Minh N. Do

***Abstract*—This paper is motivated by multichannel sampling applications. We consider a hybrid filter banks consisting of a set of fractional delays operators, slow A/D converters with different antialiasing filters, digital expanders, and digital synthesis filters (to be designed). The synthesis filters are designed to minimize the maximum gain of a hybrid induced error system. We show that the induced error system is equivalent to a digital system. This digital system enables the design of stable synthesis filters using existing control theory tools such as model-matching and linear matrix inequalities. Moreover, the induced error is robust against delay estimate errors. Numerical experiments show the proposed approach yields better performance compared to existing techniques.**

***Index Terms*—Multichannel sampling, sampled-data control, $\mathcal{H}_\infty$ optimization, model-matching, linear matrix inequality, polyphase, fractional delay, filter design, hybrid filter banks.**

I. Introduction

This paper is motivated by multichannel sampling applications. Figure 1(a) shows the model of a fast analog-to-digital (A/D) converter used to obtain a *desired* high-resolution signal. An analog input signal $f(t)$ is convolved with an antialiasing filter $\phi_0(t)$ (also known as the sampling kernel function) whose Laplace transform is $\Phi_0(s)$. The output of the convolution is then sampled at small sampling interval h. The desired high-resolution signal is denoted by $y_0[n] = (f * \phi_0)(nh)$ for $n \in \mathbb{Z}$.

Figure 1(b) depicts how *actual* low-resolution signals $\{x_i[n]\}_{i=1}^N$ are sampled using slow A/D converters. The same analog input $f(t)$ is sampled in parallel using N slow A/D converters. In the i-th channel, for $1 \le i \le N$, the input $f(t)$ is first convolved with a function $\phi_i(t)$ (with Laplace transform $\Phi_i(s)$) before being delayed by $D_i > 0$ (to compensate for different time arrivals). The low-rate signals $x_i[n] = (f * \phi_i)(nMh - D_i)$, for $n \in \mathbb{Z}$, can be used to synthesize the high-resolution signal $y_0[n]$ of Fig. 1(a).

The goal of the paper is to design an N-input M-output digital system $\boldsymbol{F}(z)$, see Fig. 2, that synthesizes the high-resolution signal $y_0[n]$ using low-resolution signals $\{x_i[n]\}_{i=1}^N$. This implementation can be done in parallel in the same clock speed of slow A/D converters; the high-rate output is obtained only at the final step by interleaving samples (also known as a polyphase transform [28], [29]). More specifically, we minimize the errors (using a criterion defined later) of a *hybrid* induced error system $\mathcal{K}$ shown in Fig. 3, where $\{F_i(z)\}_{i=1}^N$ are equivalent synthesis filters such that their $M \times N$ polyphase matrix is $\boldsymbol{F}(z)$ of Fig. 2:

$$[F_1(z) \quad F_2(z) \dots F_N(z)] = [1 \quad z^{-1} \dots z^{-M+1}]\boldsymbol{F}(z^M). \quad (1)$$

Note that the high-rate signal $y_0[n]$ is approximated with a delay of m_0 samples. Among components of $\mathcal{K}$, the transfer functions $\{\Phi_i(s)\}_{i=0}^N$ characterize antialiasing filters, and delays $\{D_i\}_{i=1}^N$ model system setup such as arrival times or sampling positions. We assume that, through construction and calibration, information about the sampling kernel functions $\{\Phi_i(s)\}_{i=0}^N$ and delays $\{D_i\}_{i=1}^N$ are available. In such case, we

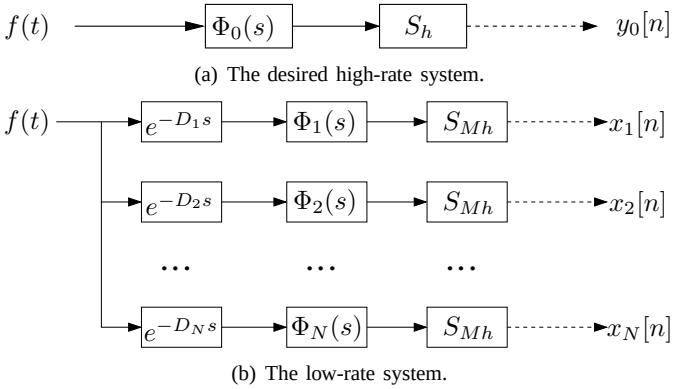

(a) The desired high-rate system.

(b) The low-rate system.

Fig. 1. (a) The desired high-rate system, (b) the low-rate system. The fast-sampled signal $y_0[n]$ can be approximated using slow-sampled signals $\{x_i[n]\}_{i=1}^N$.

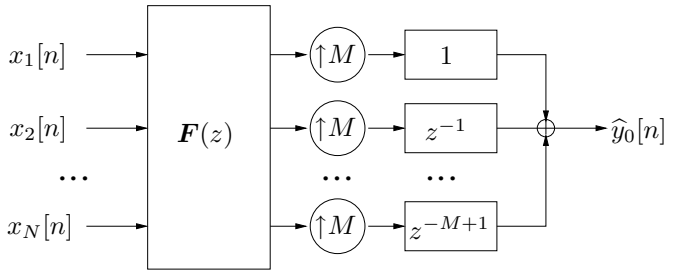

Fig. 2. Approximation of the *high-resolution* signal from *low-resolution* signals using an N-input M-output digital system $\boldsymbol{F}(z)$ and interleaving its outputs. This polyphase structure is used for its efficiency and its ability to keep the computation in low-rate.

Ha T. Nguyen is with the Department of Electrical and Computer Engineering and the Coordinated Science Laboratory, University of Illinois, Urbana IL 61801 (email: thai-ha.nguyen@m4x.org).

Minh N. Do is with the Department of Electrical and Computer Engineering, the Coordinated Science Laboratory, and the Beckman Institute, University of Illinois, Urbana IL 61801 (email: minhdo@uiuc.edu).

This work was supported by the National Science Foundation under Grant ITR-0312432.

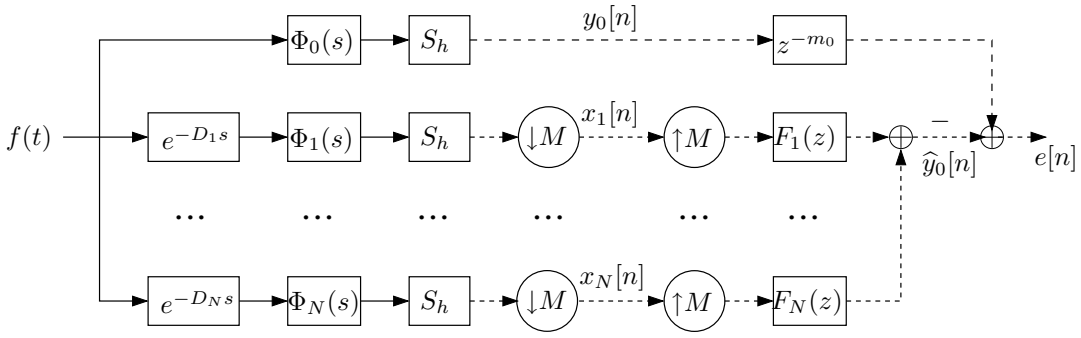

Fig. 3. The hybrid induced error system $\mathcal{K}$ with analog input $f(t)$ and digital output $e[n]$. We want to design synthesis filters $\{F_i(z)\}_{i=1}^N$ based on the transfer function $\{\Phi_i(s)\}_{i=0}^N$, the fractional delays $\{D_i\}_{i=1}^N$, the system delay tolerance m_0, the sampling interval h, and the super-resolution rate M to minimize the $\mathcal{H}_\infty$ norm of the induced error system $\mathcal{K}$. Note that the synthesis filter bank is shown here in parallel structure with filters $\{F_i(z)\}_{i=1}^N$ for symmetry, but for actual implementation it is more efficient to use polyphase structure with $\boldsymbol{F}(z)$ as shown in Fig. 2.

want to design a corresponding optimal synthesis polyphase matrix $\boldsymbol{F}(z)$, or equivalently a filter bank $\{F_i(z)\}_{i=1}^N$, so that the resulting system depicted in Fig. 3 can be subsequently put in operation for arbitrary input signals $f(t)$. A special case of this multichannel sampling setup is called *time-interleaved A/D converters* where $\Phi_i(s) = \Phi_0(s)$ and $D_i = ih$ for $i = 1, 2, \ldots, N$. Then the synthesis filter bank can simply interleave samples, i.e. $F_i(z) = z^i$. Multichannel sampling extends time-interleaved A/D converters by allowing mismatch in sampling kernels before slow A/D converters [8]. Moreover, in many cases, the time delays $\{D_i\}_{i=1}^N$, although they can be measured [2], [14], [15], [30], cannot be controlled. Under these conditions, the multichannel sampling setup studied in this paper can be ideally applied.

We note that many practical systems, such as electrical, mechanical, and electromechanical systems, can be modeled by differential equations [18, Chapter 1]. Their Laplace transforms are thus rational functions of form $A(s)/B(s)$ for some polynomials $A(s)$ and $B(s)$. In the contrary, fractional delay operators $e^{-D_i s}$ are never rational if $D_i \neq 0$, though when D_i is an integer multiple of h, operator $e^{-D_i s}$ can be pushed after the sampling operator S_h to become an integer delay (in the digital domain). Working with fractional delay operators $e^{-D_i s}$ is necessary, though nontrivial, to keep intersample behaviors of the input signals.

Problem formulation. We consider the hybrid system $\mathcal{K}$ illustrated in Fig. 3. The $\mathcal{H}_\infty$ norm of $\mathcal{K}$ is defined as

$$\|\mathcal{K}\|_\infty := \sup_{f \in L^2, f \neq 0} \left\{ \frac{\|e\|_2}{\|f\|_2} \right\}, \tag{2}$$

where $\|e\|_2$ is the l_2 norm of $e[n]$ and $\|f\|_2$ is the L_2 norm of $f(t)$. We want to design (IIR or FIR) synthesis filters $\{F_i(z)\}_{i=1}^N$ to minimize $\|\mathcal{K}\|_\infty$. The inputs of our algorithms consist of the strictly proper transfer functions $\{\Phi_i(s)\}_{i=0}^N$, the positive fractional delays $\{D_i\}_{i=1}^N$, the system delay tolerance $m_0 \geq 0$, the sampling interval $h > 0$, and the upsampling-rate $M \geq 2$.

In the design of the synthesis filter $\{F_i(z)\}_{i=1}^N$, the system performance is evaluated using the $\mathcal{H}_\infty$ approach [9], [12], [26]. In the digital-domain, we work on the Hardy space $\mathcal{H}_\infty$ that consists of all complex-value transfer matrices $\boldsymbol{G}(z)$ which are analytic and bounded outside of the unit circle $|z| > 1$. Hence $\mathcal{H}_\infty$ is the space of transfer matrices that are stable in the bounded-input bounded-output sense. The $\mathcal{H}_\infty$ norm of $\boldsymbol{G}(z)$ is defined as the maximum gain of the corresponding system. If a system $\boldsymbol{G}$, analog or digital, has input $\boldsymbol{u}$ and output $\boldsymbol{y}$, the $\mathcal{H}_\infty$ norm of $\boldsymbol{G}$ is [9]

$$\|\boldsymbol{G}\|_\infty = \sup \left\{ \|\boldsymbol{y}\|_2 : \boldsymbol{y} = \boldsymbol{G}\boldsymbol{u}, \|\boldsymbol{u}\|_2 = 1 \right\}, \tag{3}$$

where the norms are regular Euclidean norm $\|\cdot\|$; that is,

$$\|\boldsymbol{x}\|_2 = \left(\sum_{n=-\infty}^{\infty} \|\boldsymbol{x}[n]\|^2 \right)^{1/2}$$

for digital signals $\boldsymbol{x}[n]$, and

$$\|\boldsymbol{x}\|_2 = \left(\int_{-\infty}^{\infty} \|\boldsymbol{x}(t)\|^2 dt \right)^{1/2}$$

for analog signals $\boldsymbol{x}(t)$.

The use of $\mathcal{H}_\infty$ optimization framework, originally proposed by Shenoy et al. [25] for filter bank designs, offers powerful tools for signal processing problems. In our case, using the $\mathcal{H}_\infty$ optimization framework, the induced error is uniformly small over all finite energy inputs $f(t) \in \mathcal{L}_2(\mathbb{R})$ (i.e., $\|f(t)\|_2 < \infty$). Furthermore, no assumptions of $f(t)$, such as band-limitedness, are necessary. We minimize the worst induced error over all finite energy inputs $f(t)$. This is important since many practical signals are not bandlimited such as images with discontinuities at edges [27]. Finally, since $\mathcal{H}_\infty$ optimization is performed in the Hardy space, the designed filters are guaranteed to be stable.

The paper's main contributions are twofold. First, we use sampled-data control techniques to convert the design problem for $\mathcal{K}$ into a $\mathcal{H}_\infty$ norm equivalent finite-dimensional model-matching problem. The conversion enables the design synthesis filters, IIR or FIR, to minimize the $\mathcal{H}_\infty$ norm of $\mathcal{K}$. The norm equivalence property reduces the induced errors compared to methods that approximate the fractional delays by IIR or FIR filters [17], [24], [32], [16]. IIR synthesis filters are designed using available solutions to the model-matching problem [9], [12]. To design FIR filters, we use linear matrix inequality (LMI) methods [1], [3]. Although FIR filter designs using LMI methods have been proposed for other problems [31], [21], [22], to our knowledge, only IIR filter

designs are proposed for related problems [23], [14], [26], [4]. The second main contribution, shown in Section V, is the robustness of the designed induced error system $\mathcal{K}$ against delay estimate errors.

Related work. Herley and Wong addressed the problem of the sampling and reconstruction of an analog signal from a periodic nonuniform set of samples assuming that the input signals have fixed frequency support [13]. Marziliano and Vetterli also addressed the problem of reconstructing a digital signal from a periodic nonuniform set of samples using Fourier transform [20]. However, in both cases, the authors only considered a restricted set of input signals that are bandlimited. Moreover, they only considered *rational* delays, that is, the set of samples is the set left after discarding a uniform set of samples in a periodic fashion (the ratio between the delays and the sample intervals is a rational number, hence the name rational delays). Jahromi and Aarabi considered the problem of estimating the delays $\{D_i\}_{i=1}^N$ and of designing analysis and synthesis filters to minimize the $\mathcal{H}_\infty$ norm of an induced error system [14]. However, the authors only considered integer delays or *approximation* of fractional delays by IIR or FIR filters. Shu et al. addressed the problem of designing the synthesis filters for a filter bank to minimize the $\mathcal{H}_\infty$ norm of an induced system [26]. Their problem was similar to the problem considered in this paper, except that it did not consider the fractional delays but a rational transfer function instead. Nagahara et al. synthesized IIR and FIR filters to approximate fractional delays using $\mathcal{H}_\infty$ optimization [21], [22]. Although their problem is not multirate, the result therein can be considered as a special case of our problem when $M = N = 1$.

Throughout this paper, we adopt the following conventions. An (analog or digital) single-input single-output transfer function G is written in regular font, an (analog or digital) multi-input and/or multi-output $\boldsymbol{G}$ is written in bold, and a hybrid system $\mathcal{G}$ is written in calligraphic font. The notation

$$\boldsymbol{G} = \left[\begin{array}{c|c} A & B \\ \hline C & D \end{array}\right] \quad \text{or} \quad G = \{A, B, C, D\} \tag{4}$$

is used to denote a state-space representation of a system $\boldsymbol{G}$, that is $\boldsymbol{G}(s) = D + C(sI - A)^{-1}B$ for an analog system or $\boldsymbol{G}(z) = D+C(zI-A)^{-1}B$ for a digital system [12]. We write scalars in regular font as x, and vectors in bold as $\boldsymbol{x}$. In our figures, solid lines illustrate analog signals, and dashed lines are intended for digital ones. We denote S_h for the sampling operator by h; i.e. $S_h\{v(t)\}[n] = v(nh)$.

The remainder of this paper is organized as follows. In Section II, we show that the design problem is equivalent to a model-matching problem. Design procedures for IIR and FIR synthesis filters are presented in Section III and IV, respectively. Robustness of the designed system against delay estimates is presented in Section V. We show experimental results in Section VI. Finally, we give conclusion and discussion in Section VII.

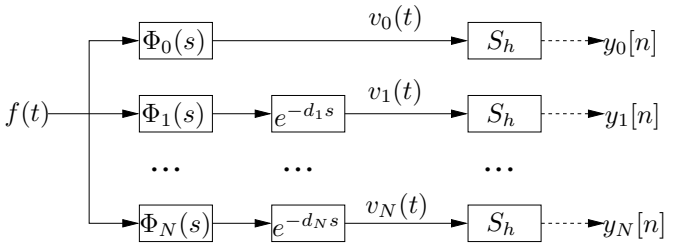

Fig. 4. The hybrid (analog input digital output) subsystem $\mathcal{G}$ of $\mathcal{K}$. Note that the sampling interval of all channels is h.

II. Equivalence of $\mathcal{K}$ to a Model-Matching Problem

In this section, we show that there exists a finite-dimensional digital linear time-invariant system $\boldsymbol{K}$ that has the same $\mathcal{H}_\infty$ norm with $\mathcal{K}$. We demonstrate this in three steps. In Section II-A, we convert $\mathcal{K}$ into an infinite-dimensional digital system. Next, in Section II-B, we convert the system further into a finite-dimensional system $\boldsymbol{K}_d$. Finally, in Section II-C, we convert $\boldsymbol{K}_d$ into a linear time-invariant system.

A. Equivalence of $\mathcal{K}$ to a digital system

The idea is to show that the hybrid subsystem $\mathcal{G}$ (see Fig. 4) of $\mathcal{K}$ is $\mathcal{H}_\infty$ norm equivalent to a digital system. In Fig. 4, we denote $\{d_i\}_{i=1}^N$ the fractional parts of $\{D_i\}_{i=1}^N$. In other words, we have $0 \le d_i < h$ and $m_i \in \mathbb{Z}$ such that

$$D_i = m_i h + d_i \quad (1 \le i \le N). \tag{5}$$

In our mathematical derivation, m_i, and hence D_i, for $1 \le i \le N$, can be negative, though in many practical applications, D_i are strictly greater than zero. Note that by working with system $\mathcal{G}$, we need to compensate for the difference between $e^{-D_i s}$ and $e^{-d_i s}$. These differences are analog delay operators $e^{-m_i h s}$ that can be *interchanged* with the sampling operators S_h to produce digital integer delay operators z^{-m_i}.

To find a $\mathcal{H}_\infty$ norm equivalent digital system for $\mathcal{G}$, we adopt a divide-and-conquer approach: each channel of $\mathcal{G}$ will be shown to be $\mathcal{H}_\infty$ norm equivalent to a digital system. Since $\Phi_0(s)$ is strictly proper, there exist state-space matrices $\{A_0, B_0, C_0, 0\}$ and state function $\boldsymbol{x}_0(t)$ such that

$$\left\{\begin{array}{rcl} \dot{\boldsymbol{x}}_0(t) &=& A_0\boldsymbol{x}_0(t) + B_0 f(t) \\ v_0(t) &=& C_0\boldsymbol{x}_0(t). \end{array}\right.$$

For $0 \le t_1 < t_2 < \infty$, we can compute the future state value $\boldsymbol{x}_0(t_2)$ from a previous state value $\boldsymbol{x}_0(t_1)$ as follows:

$$\boldsymbol{x}_0(t_2) = e^{(t_2-t_1)A_0}\boldsymbol{x}_0(t_1) + \int_{t_1}^{t_2} e^{(t_2-\tau)A_0}B_0 f(\tau)d\tau. \tag{6}$$

Define linear operator $\boldsymbol{Q}_0$ taking inputs $u(t) \in \mathcal{L}_2[0, h)$ as

$$\boldsymbol{Q}_0 u = \int_0^h e^{(h-\tau)A_0}B_0 u(\tau)d\tau. \tag{7}$$

Applying (6) using $t_1 = nh$ and $t_2 = (n+1)h$ we get

$$\boldsymbol{x}_0((n+1)h) = e^{hA_0}\boldsymbol{x}_0(nh) + \boldsymbol{Q}_0\widetilde{f}[n], \tag{8}$$

where $\widetilde{f}[n]$ denotes the portion of $f(t)$ on the interval $[nh, nh+h)$ translated to $[0,h)$. In other words, we consider the analog signal $f(t)$ as a sequence $\{\widetilde{f}[n]\}_{n\in\mathbb{Z}}$ with $\widetilde{f}[n] \in \mathcal{L}_2[0,h)$. The mapping from $f(t)$ into $\{\widetilde{f}[n]\}_{n\in\mathbb{Z}}$ is called the *lifting* operator [5, Section 10.1]. Clearly, the lifting operator preserves the energy of the signals, that is,

$$\|f(t)\|_2 = \|\widetilde{f}\|_2 = \left(\sum_{n=-\infty}^{\infty} \|\widetilde{f}[n]\|_2^2\right)^{1/2},$$

where $\|\widetilde{f}[n]\|_2^2 := \int_{nh}^{(n+1)h} |f(t)|^2 dt$.

Let $\mathcal{G}_0$ be the hybrid subsystem of $\mathcal{G}$ with input $f(t)$ and output $y_0[n]$ (see Fig. 4). An implication of (8) is that $y_0[n] = v_0(nh)$ can be considered as the output of a digital system with input $\widetilde{f}[n]$ and state $\boldsymbol{x}_{d0}[n] = \boldsymbol{x}_0(nh)$ as follows:

$$\left\{\begin{array}{rcl} \boldsymbol{x}_{d0}[n+1] &=& e^{hA_0}\boldsymbol{x}_{d0}[n] + \boldsymbol{Q}_0\widetilde{f}[n] \\ y_0[n] &=& C_0\boldsymbol{x}_{d0}[n]. \end{array}\right.$$

Since the lifting operator preserves the norm, system $\mathcal{G}_0$ is $\mathcal{H}_\infty$ norm equivalent to the system $\boldsymbol{G}_0 = \{e^{hA_0}, \boldsymbol{Q}_0, C_0, 0\}$.

The same technique can be used for the remaining channels. Let $\mathcal{G}_i$, for $1 \le i \le N$, be the hybrid subsystem of $\mathcal{G}$ with input $f(t)$ and output $y_i[n]$ (see Fig. 4). Suppose that $\{A_i, B_i, C_i, 0\}$ is a state-space realization of $\Phi_i(s)$ with state function $\boldsymbol{x}_i(t)$. We define linear operators $\boldsymbol{Q}_i$ and $\boldsymbol{R}_i$ taking inputs $u(t) \in \mathcal{L}_2[0,h)$ as

$$\boldsymbol{Q}_i u = \int_0^h e^{(h-\tau)A_i} B_i u(\tau) d\tau, \tag{9}$$

and

$$\boldsymbol{R}_i u = C_i \int_0^{h-d_i} e^{(h-d_i-\tau)A_i} B_i u(\tau) d\tau. \tag{10}$$

Similar to (8), we can obtain

$$\boldsymbol{x}_i((n+1)h) = e^{hA_i}\boldsymbol{x}_i(nh) + \boldsymbol{Q}_i\widetilde{f}[n]. \tag{11}$$

Applying (6) again with $t_1 = nh$ and $t_2 = (n+1)h - d_i$ we get

$$\begin{aligned}\boldsymbol{x}_i((n+1)h - d_i) = e^{(h-d_i)A_i}\boldsymbol{x}_i(nh) + \\ + \int_{nh}^{(n+1)h-d_i} e^{((n+1)h-d_i-\tau)A_i} B_i f(\tau) d\tau.\end{aligned}$$

Since $v_i(t) = C_i\boldsymbol{x}_i(t-d_i)$ for all t, using $t = (n+1)h$ we obtain

$$v_i((n+1)h) = C_i e^{(h-d_i)A_i}\boldsymbol{x}_i(nh) + \boldsymbol{R}_i\widetilde{f}[n]. \tag{12}$$

From (11) and (12) we see that $y_i[n] = v_i(nh)$ can be considered as the output of a digital system with input $\widetilde{f}[n]$ and state $\boldsymbol{x}_{di}[n] = \begin{bmatrix} \boldsymbol{x}_i(nh) \\ v_i(nh) \end{bmatrix}$ as follows:

$$\left\{\begin{array}{rcl} \boldsymbol{x}_{di}[n+1] &=& \underbrace{\begin{bmatrix} e^{hA_i} & 0 \\ C_i e^{(h-d_i)A_i} & 0 \end{bmatrix}}_{A_{di}} \boldsymbol{x}_{di}[n] + \underbrace{\begin{bmatrix} \boldsymbol{Q}_i \\ \boldsymbol{R}_i \end{bmatrix}}_{\boldsymbol{B}_i} \widetilde{f}[n] \\ y_i[n] &=& \underbrace{[\boldsymbol{0}, 1]}_{C_{di}} \boldsymbol{x}_{di}[n]. \end{array}\right. \tag{13}$$

Since the lifting operator preserves the norm, system $\mathcal{G}_i$ is $\mathcal{H}_\infty$ norm equivalent to the system $\boldsymbol{G}_i = \{A_{di}, \boldsymbol{B}_i, C_{di}, 0\}$.

Finally, we note that the system $\mathcal{G}$ is the vertical concatenation of subsystems $\{\mathcal{G}_i\}_{i=0}^N$. Since each subsystem $\mathcal{G}_i$ is $\mathcal{H}_\infty$ norm equivalent to the system $\boldsymbol{G}_i$ with the same input $\widetilde{f}[n]$, for $0 \le i \le N$, the system $\mathcal{G}$ is also $\mathcal{H}_\infty$ norm equivalent to the vertical concatenation system $\boldsymbol{G}$ of subsystems $\{\boldsymbol{G}_i\}_{i=0}^N$. We summarize the result of this Section in Proposition 1.

Proposition 1: The system $\mathcal{G}$ is $\mathcal{H}_\infty$ norm equivalent to the infinite-dimensional digital system

$$\boldsymbol{G} = \left[\begin{array}{c|c} A_d & \boldsymbol{B} \\ \hline C_d & 0 \end{array}\right], \tag{14}$$

where $A_d, \boldsymbol{B}, C_d$ are determined as

$$\left\{\begin{array}{rcl} A_d &=& \mathrm{diag}_{N+1}\left(e^{hA_0}, A_{d1}, \ldots, A_{dN}\right) \\ \boldsymbol{B} &=& [\boldsymbol{Q}_0^T \quad \boldsymbol{B}_1^T \quad \ldots \quad \boldsymbol{B}_N^T]^T \\ C_d &=& \mathrm{diag}_{N+1}(C_0, [\boldsymbol{0}, 1], \ldots, [\boldsymbol{0}, 1]). \end{array}\right. \tag{15}$$

In the above equations, and in the remainder of the paper, we denote $\mathrm{diag}_k(\alpha_1, \alpha_2, \ldots, \alpha_k)$ the matrix with α_i in the diagonal, for $1 \le i \le k$, and 0 elsewhere, where $\{\alpha_i\}_{i=1}^k$ can be scalars, vectors, or matrices.

B. Equivalence of $\mathcal{K}$ to a finite-dimensional digital system

Proposition 1 shows that $\mathcal{G}$ is $\mathcal{H}_\infty$ norm equivalent to an infinite-dimensional digital system $\boldsymbol{G}$. Next, we convert $\boldsymbol{G}$ further into some finite-dimensional digital system $\boldsymbol{G}_d$.

Proposition 2: Let $\boldsymbol{B}^*$ be the adjoint operator of $\boldsymbol{B}$ and B_d be a square matrix such that

$$B_d B_d^T = \boldsymbol{B}\boldsymbol{B}^*. \tag{16}$$

The finite-dimensional digital system $\boldsymbol{G}_d(z) \Leftrightarrow \{A_d, B_d, C_d, 0\}$ has the same $\mathcal{H}_\infty$ norm with $\mathcal{G}$:

$$\|\boldsymbol{G}_d\|_\infty = \|\mathcal{G}\|_\infty. \tag{17}$$

Proof: The product $\boldsymbol{B}\boldsymbol{B}^*$ is a linear operator characterized by a square matrix of finite dimension (the computation of $\boldsymbol{B}\boldsymbol{B}^*$ is given in Appendix). Hence $\boldsymbol{G}_d(z) \Leftrightarrow \{A_d, B_d, C_d, 0\}$ is a finite-dimensional digital system. The proof of (17) can be found in [5, Section 10.5]. ■

Proposition 2 claims that, for all analog signals $f(t)$, there exists a digital signal $\boldsymbol{u}[n]$ having the same energy as $f(t)$ such that $[y_0, \ldots, y_N]^T = \boldsymbol{G}_d\boldsymbol{u}$. The dimension n_u of $\boldsymbol{u}[n]$ is equal to the number of rows of A_d (see Proposition 1), i.e.,

$$n_u = n_0 + n_1 + \ldots + n_N + N, \tag{18}$$

where n_i is the number of rows of A_i, for $0 \le i \le N$. Since we want to minimize the worst induced error over all inputs $f(t)$ of finite energy, we also need to minimize $\|\boldsymbol{G}_d\|_\infty$ for all inputs $\boldsymbol{u}[n]$ (having the same energy with $f(t)$).

At this point, we take into account the integer delay operators $\{z^{-m_i}\}_{i=0}^N$ to obtain a digital system $\boldsymbol{K}_d$ that has the same $\mathcal{H}_\infty$ norm as $\mathcal{K}$.

Proposition 3: Let C_{di} be the i-th row of the $(N+1)$-row matrix C_d (see Proposition 1), and $\boldsymbol{H}_i(z)$ be the multi-input

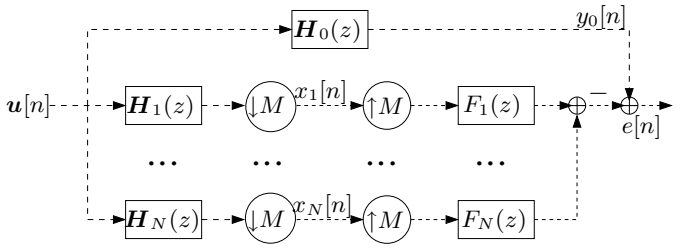

Fig. 5. The $\mathcal{H}_\infty$ norm equivalent digital system $\boldsymbol{K}_d$ of $\mathcal{K}$ (see Proposition 3). Here $\{\boldsymbol{H}_i(z)\}_{i=0}^N$ are rational transfer functions defined in (19). Note that the input $\boldsymbol{u}[n]$ is of n_u dimension.

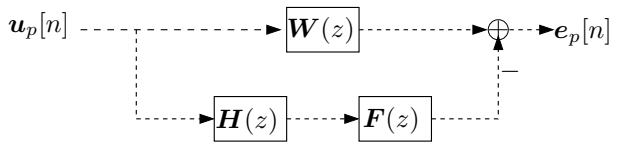

Fig. 6. The equivalent LTI error system $\boldsymbol{K}(z)$ (see Theorem 1). Note that the system $\boldsymbol{K}(z)$ is Mn_u input M output, the transfer matrices $\boldsymbol{W}(z), \boldsymbol{H}(z)$ are of dimension $M \times Mn_u$, and $\boldsymbol{F}(z)$ is of dimension $M \times M$.

single-output rational function that outputs $y_i[n]$ from input $\boldsymbol{u}[n]$, for $0 \le i \le N$. The system $\boldsymbol{H}_i(z)$ can be computed as

$$\boldsymbol{H}_i(z) = z^{-m_i} \left[\begin{array}{c|c} A_d & B_d \\ \hline C_{di} & 0 \end{array}\right] \quad (0 \le i \le N). \tag{19}$$

As a result, system $\mathcal{K}$ is equivalent to the multiple-input one-output digital system $\boldsymbol{K}_d(z)$ illustrated in Fig. 5.

C. Equivalence of $\mathcal{K}$ to a linear time-invariant system

The finite-dimensional digital system $\boldsymbol{K}_d$ is not linear time-invariant (LTI) because of the presence of upsampling and downsampling operators $(\uparrow M), (\downarrow M)$. We apply polyphase techniques [28], [29] to make $\boldsymbol{K}_d$ an LTI system.

Let $\boldsymbol{H}_{0,j}(z)$, for $0 \le j \le M-1$, be the polyphase components of filter $\boldsymbol{H}_0(z)$. In other words,

$$\boldsymbol{H}_0(z) = \sum_{j=0}^{M-1} z^j \boldsymbol{H}_{0,j}(z^M). \tag{20}$$

We also denote $\boldsymbol{u}_p[n]$ and $\boldsymbol{e}_p[n]$ the polyphase versions of $\boldsymbol{u}[n]$ and $e[n]$. Note that $\|\boldsymbol{u}_p\|_2 = \|\boldsymbol{u}\|_2$ and $\|\boldsymbol{e}_p\|_2 = \|e\|_2$. Hence, by working in the polyphase domain, $\boldsymbol{K}_d(z)$ is converted into an LTI system with the same $\mathcal{H}_\infty$ norm.

Proposition 4: The digital error system $\boldsymbol{K}_d(z)$ is equivalent to the LTI system

$$\boldsymbol{K}(z) = \boldsymbol{W}(z) - \boldsymbol{H}(z)\boldsymbol{F}(z) \tag{21}$$

with input $\boldsymbol{u}_p[n]$ and output $\boldsymbol{e}_p[n]$. In (21), $\boldsymbol{H}(z)$ and $\boldsymbol{F}(z)$ are standard polyphase matrices of $\{\boldsymbol{H}_i(z)\}_{i=1}^N$ and $\{\boldsymbol{F}_i(z)\}_{i=1}^N$, and

$$(\boldsymbol{W}(z))_{i,j} = \begin{cases} \boldsymbol{H}_{0,j-i}(z) & \text{if } 1 \le i \le j \le M \\ z\boldsymbol{H}_{0,M+j-i}(z) & \text{if } 1 \le j < i \le M. \end{cases} \tag{22}$$

Proof: The proof uses standard polyphase techniques [28], [29], hence omitted here. ∎

Figure 6 shows the equivalent digital, LTI error system $\boldsymbol{K}(z)$. The transfer function matrix $\boldsymbol{F}(z)$ is to be designed.

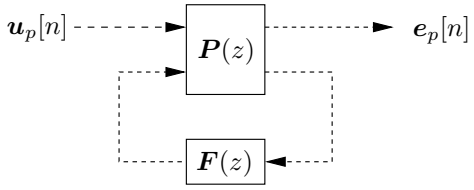

Fig. 7. The induced error system $\boldsymbol{K}(z)$ of the form of the standard problem in $\mathcal{H}_\infty$ control theory with input $\boldsymbol{u}_p[n]$ output $\boldsymbol{e}_p[n]$. We want to design synthesis system $\boldsymbol{F}(z)$ to minimize $\|\boldsymbol{K}\|_\infty$.

State-space realizations of $\boldsymbol{H}(z)$ and $\boldsymbol{W}(z)$ are given in Theorem 1 using state-space realizations $\{A_{\boldsymbol{H}_i}, B_{\boldsymbol{H}_i}, C_{\boldsymbol{H}_i}, 0\}$ of $\{\boldsymbol{H}_i(z)\}_{i=0}^N$ (it can be easily verified that the D-matrix of $\boldsymbol{H}_i(z)$ is a zero-matrix).

Theorem 1: The original induced error system $\mathcal{K}$ has an $\mathcal{H}_\infty$ norm equivalent digital, LTI system $\boldsymbol{K}(z) = \boldsymbol{W}(z) - \boldsymbol{F}(z)\boldsymbol{H}(z)$ (see Fig. 6); that is,

$$\|\mathcal{K}\|_\infty = \|\boldsymbol{W}(z) - \boldsymbol{F}(z)\boldsymbol{H}(z)\|_\infty, \tag{23}$$

where $\boldsymbol{F}(z)$ is the polyphase matrix of $\{F_i(z)\}_{i=1}^N$ to be designed. State-space realizations of $\boldsymbol{W}(z)$ and $\boldsymbol{H}(z)$ can be computed as follows:

$$\begin{array}{lcl} A_W & = & A_{\boldsymbol{H}_0}^M \\ B_W & = & [A_{\boldsymbol{H}_0}^{M-1} B_{\boldsymbol{H}_0},\ A_{\boldsymbol{H}_0}^{M-2} B_{\boldsymbol{H}_0}, \ldots,\ B_{\boldsymbol{H}_0}] \\ C_W & = & [(C_{\boldsymbol{H}_0})^T,\ (C_{\boldsymbol{H}_0} A_{\boldsymbol{H}_0})^T, \ldots,\ (C_{\boldsymbol{H}_0} A_{\boldsymbol{H}_0}^{M-1})^T]^T \\ (D_W)_{ij} & = & \begin{cases} C_{\boldsymbol{H}_0} A_{\boldsymbol{H}_0}^{i-j-1} B_{\boldsymbol{H}_0} & \text{if } 1 \le j < i \le M, \\ 0 & \text{else} \end{cases} . \end{array} \tag{24}$$

and

$$\begin{array}{lcl} A_H & = & \mathrm{diag}_N(A_{\boldsymbol{H}_1}^M, \ldots, A_{\boldsymbol{H}_1}^M) \\ (B_H)_{ij} & = & A_{\boldsymbol{H}_i}^{M-j} B_{\boldsymbol{H}_i}, \quad \text{for } 1 \le i \le N, 1 \le j \le M \\ C_H & = & \mathrm{diag}_N(C_{\boldsymbol{H}_1}, \ldots, C_{\boldsymbol{H}_N}) \\ D_H & = & \boldsymbol{0}. \end{array} \tag{25}$$

Proof: We give here the proof for (24). The proof for Eq. (25) can be derived similarly. Consider the transfer function $\boldsymbol{H}_{00}(z)$ in the block $(1,1)$ of $\boldsymbol{W}(z)$ (see Proposition 4):

$$\begin{array}{lcl} \boldsymbol{H}_{00}(z) & = & \displaystyle\sum_{i=1}^{\infty} C_{\boldsymbol{H}_0} A_{\boldsymbol{H}_0}^{iM-1} B_{\boldsymbol{H}_0} z^{-i} \\ & = & \displaystyle\sum_{i=1}^{\infty} C_{\boldsymbol{H}_0} \left(A_{\boldsymbol{H}_0}^M\right)^{i-1} \left(A_{\boldsymbol{H}_0}^{M-1} B_{\boldsymbol{H}_0}\right) z^{-i} \\ & = & \left[\begin{array}{c|c} A_{\boldsymbol{H}_0}^M & A_{\boldsymbol{H}_0}^{M-1} B_{\boldsymbol{H}_0} \\ \hline C_{\boldsymbol{H}_0} & 0 \end{array}\right]. \end{array}$$

The state-space representation of the block $(1,1)$ of $\boldsymbol{W}(z)$ is in agreement with (24). The same technique can be applied for the remaining blocks. ∎

III. Design of IIR Filters

A. Conversion to the standard $\mathcal{H}_\infty$ control problem

The problem of designing $\boldsymbol{F}(z)$ to minimize $\|\boldsymbol{K}\|_\infty$ (see Fig. 6) has a similar form to the model-matching form which is a special case of the *standard problem* in $\mathcal{H}_\infty$ control

theory [9], [12]. Figure 7 shows the system $\boldsymbol{K}(z)$ in the standard form. The system $\boldsymbol{P}(z)$ of Fig. 7 has a state-space realization derived from ones of $\boldsymbol{W}(z)$ and $\boldsymbol{H}(z)$ as

$$\left[\begin{array}{c|c} A_P & B_P \\ \hline C_P & D_P \end{array}\right] = \left[\begin{array}{cc|cc} A_W & 0 & B_W & 0 \\ 0 & A_H & B_H & 0 \\ \hline C_W & 0 & D_W & -I \\ 0 & C_H & D_H & 0 \end{array}\right]. \quad (26)$$

Solutions to the standard problem have existing software, such as MATLAB's Robust Control Toolbox [6], to facilitate the optimization procedures.

B. Design procedure

- **Inputs:** Rational transfer functions $\{\Phi_i(s)\}_{i=0}^N$ (strictly proper), positive fractional delays $\{D_i\}_{i=1}^N$, the system tolerance delay $m_0 \geq 0$, the sampling interval $h > 0$, the superresolution rate $M \geq 2$.
- **Outputs:** IIR synthesis filters $\{F_i(z)\}_{i=1}^N$ or equivalently polyphase matrix $\boldsymbol{F}(z)$.

1) Let $D_i = m_i h + d_i$ for $1 \leq i \leq N$ as in (5).
2) Compute a state-space realization $\{A_i, B_i, C_i, 0\}$ of $\Phi_i(s)$ for $0 \leq i \leq N$.
3) Compute the system $\boldsymbol{G}_d = \{A_d, B_d, C_d, 0\}$ as in Proposition 1 and 2.
4) Compute a state-space realization of $\boldsymbol{H}_i(z)$, for $0 \leq i \leq N$, as in Proposition 3.
5) Compute the state-space realization of $\boldsymbol{W}(z)$ and $\boldsymbol{H}(z)$ as in (24) and in (25) of Theorem 1.
6) Compute the state-space realization of $\boldsymbol{P}(z)$ from $\boldsymbol{H}(z)$ and $\boldsymbol{W}(z)$ as in (26).
7) Design a synthesis system $\boldsymbol{F}(z)$ using existing $\mathcal{H}_\infty$ optimization tools.

IV. Design of FIR Filters

A. Conversion to a linear matrix inequality problem

In this section, we present a design procedure to synthesize FIR filters $\{F_i(z)\}_{i=1}^N$. For some practical applications, FIR filters are preferred to IIR filters for their robustness to noise and computational advantages.

We first derive a state-space realization $\{A_F, B_F, C_F, D_F\}$ of the polyphase matrix $\boldsymbol{F}(z)$ of $\{F_i(z)\}_{i=1}^N$ based on the coefficients of $\{F_i(z)\}_{i=1}^N$. Assuming that the synthesis FIR filters $\{F_i(z)\}_{i=1}^N$ are of maximum length $nM > 0$, for $1 \leq i \leq N$, we denote

$$F_i(z) = d_{i0} + d_{i1}z^{-1} + d_{i2}z^{-2} + \ldots + d_{i,nM-1}z^{-nM+1},$$

and

$$C_{ij} = [d_{i,j+M} \quad d_{i,j+2M} \quad \ldots \quad d_{i,j+(n-1)M}].$$

The polyphase system $\boldsymbol{F}(z)$ of $\{F_i(z)\}_{i=1}^N$ has a state-space realization $\{A_F, B_F, C_F, D_F\}$ as

$$\left\{\begin{array}{lcll} A_F & = & \mathrm{diag}_M(A_n, \ldots, A_n) & \\ B_F & = & \mathrm{diag}_M(B_n, \ldots, B_n) & \\ (C_F)_{ij} & = & C_{ji} & (0 \leq i \leq M-1 \text{ and } 1 \leq j \leq N) \\ (D_F)_{ij} & = & d_{ji} & (0 \leq i \leq M-1 \text{ and } 1 \leq j \leq N), \end{array}\right. \quad (27)$$

where matrix $A_n \in \mathbb{R}^{n \times n}$ and vector $B_n \in \mathbb{R}^n$ are

$$A_n = \left[\begin{array}{cccc} 0 & \cdots & \cdots & 0 \\ 1 & \ddots & & \vdots \\ \vdots & \ddots & \ddots & \vdots \\ 0 & \cdots & 1 & 0 \end{array}\right], \quad B_n = \left[\begin{array}{c} 1 \\ 0 \\ \vdots \\ 0 \end{array}\right].$$

Note that, given the number n, the matrices A_F, B_F do not depend on $\{F_i(z)\}_{i=1}^N$. Hence, designing $\{F_i(z)\}_{i=1}^N$ is equivalent to finding the matrices C_F, D_F to minimize $\boldsymbol{K}(z)$. The system $\boldsymbol{K}(z)$ has a state-space realization $\{A_K, B_K, C_K, D_K\}$ as follows:

$$\boldsymbol{K} = \left[\begin{array}{ccc|c} A_W & 0 & 0 & B_W \\ 0 & A_H & 0 & B_H \\ 0 & B_F C_H & A_F & B_F D_H \\ \hline C_W & -D_F C_H & -C_F & D_W - D_F D_H \end{array}\right]. \quad (28)$$

We observe that the state-space matrices of $\boldsymbol{K}(z)$ depend on C_F, D_F in a linear fashion. Hence we can use the linear matrix inequalities (LMI) [3], [10] techniques to solve for the matrices C_F, D_F.

Proposition 5: [22], [10] For a given $\gamma > 0$, the system $\boldsymbol{K}(z)$ satisfies $\|\boldsymbol{K}\|_\infty < \gamma$ if and only if there exists a positive definite matrix $P > 0$ such that

$$\left[\begin{array}{ccc} A_K^T P A_K - P & A_K^T P B_K & C_K^T \\ B_K^T P A_K & B_K^T P B_K - \gamma I & D_K^T \\ C_K & D_K & -\gamma I \end{array}\right] < 0. \quad (29)$$

For any $\gamma > 0$, Proposition 5 provides us with a tool to test if $\|\boldsymbol{K}\|_\infty < \gamma$. Hence, we can iteratively decrease γ until we get close to the optimal performance (within a predefined performance tolerance). Available implementations such as MATLAB's *LMI Control Toolbox* [11] can facilitate the design procedure.

B. Design procedure

- **Inputs:** Rational transfer functions $\{\Phi_i(s)\}_{i=0}^N$ (strictly proper), positive fractional delays $\{D_i\}_{i=1}^N$, the system tolerance delay $m_0 \geq 0$, the sampling interval $h > 0$, the superresolution rate $M \geq 2$.
- **Outputs:** FIR synthesis filters $\{F_i(z)\}_{i=1}^N$ or equivalently polyphase matrix $\boldsymbol{F}(z)$.

1) Let $D_i = m_i h + d_i$, for $1 \leq i \leq N$, as in (5).
2) Compute a state-space realization $\{A_i, B_i, C_i, 0\}$ of $\Phi_i(s)$ for $0 \leq i \leq N$.
3) Compute the system $\boldsymbol{G}_d = \{A_d, B_d, C_d, 0\}$ as in Proposition 1 and 2.
4) Compute a state-space realization of $\boldsymbol{H}_i(z)$, for $0 \leq i \leq N$, as in Proposition 3.
5) Compute the state-space realization of $\boldsymbol{W}(z)$ and $\boldsymbol{H}(z)$ as in (24) and in (25) of Theorem 1.
6) Design a synthesis system $\boldsymbol{F}(z)$ using Proposition 5.

V. Robustness against Delay Uncertainties

The proposed design procedures for synthesis filters assume perfect knowledge of the delays $\{D_i\}_{i=1}^N$. In this section, we show that the induced error system $\mathcal{K}$ obtains nearly optimal

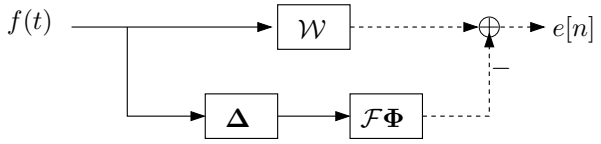

Fig. 8. The hybrid system $\mathcal{K}$ and the uncertainty operator $\boldsymbol{\Delta}$ caused by delay estimate errors.

performance if the synthesis filters are designed using estimates $\{\widehat{D}_i\}_{i=1}^N$ sufficiently close to the actual delays $\{D_i\}_{i=1}^N$.

We denote $\{\delta_i\}_{i=1}^N$ the delay jitters

$$\delta_i = D_i - \widehat{D}_i, \quad i = 1, 2, \ldots, N, \tag{30}$$

and $\overline{\delta}$ be the maximum jitter

$$\overline{\delta} = \max_{i=1}^{N}\{|\delta_i|\}. \tag{31}$$

For convenience, we also define operators

$$\begin{aligned} \boldsymbol{\Delta}(s) &= \mathrm{diag}_N(e^{-\delta_1 s}, \ldots, e^{-\delta_N s}), & (32)\\ \boldsymbol{\Phi}(s) &= \mathrm{diag}_N(\Phi_1(s), \ldots, \Phi_N(s)). & (33) \end{aligned}$$

The induced error system $\mathcal{K}$, see Fig. 3, can be rewritten as in Fig. 8, where $\mathcal{W}$ represents the high-resolution channel of $\mathcal{K}$, and $\mathcal{F}$ signifies the hybrid MIMO system composed of the delay operators $\{e^{-\widehat{D}_i s}\}_{i=1}^N$, the sampling operators S_{Mh}, the synthesis filters $\{F_i(z)\}_{i=1}^N$, and the summation of all the low resolution channels. The uncertainty operator $\boldsymbol{\Delta}$ only affects the low-resolution channels:

$$\mathcal{K} = \mathcal{W} - \mathcal{F}\boldsymbol{\Phi}\boldsymbol{\Delta}. \tag{34}$$

It is easy to see that all the operators of the above equation, in particular $\mathcal{F}$, have bounded $\mathcal{H}_\infty$ norm. Let $\overline{\omega} \in \mathbb{R}^+$ be an arbitrary, but fixed, positive number. The following Lemma gives a bound for the singular values of $\boldsymbol{I} - \boldsymbol{\Delta}(j\omega)$ and $\boldsymbol{\Phi}(j\omega)$ for each frequency ω.

Lemma 1: The maximum singular value of $\boldsymbol{I} - \boldsymbol{\Delta}(j\omega)$ and $\boldsymbol{\Phi}(j\omega)$ can be bounded as

$$\sigma_{\max}[\boldsymbol{I} - \boldsymbol{\Delta}(j\omega)] \le \sqrt{2\overline{\delta}|\omega|}, \tag{35}$$

and

$$\begin{cases} \sigma_{\max}[\boldsymbol{\Phi}(j\omega)] \le C_\Phi/\sqrt{|\omega|} & \text{if } |\omega| > \overline{\omega} \\ \sigma_{\max}[\boldsymbol{\Phi}(j\omega)] \le C_\Phi & \text{if } |\omega| \le \overline{\omega}, \end{cases} \tag{36}$$

where C_Φ is a constant depending on $\overline{\omega}$ and $\{\Phi_i\}_{i=1}^N$.

Proof: To show (35), observe that

$$\begin{aligned} \big(\boldsymbol{I} - \boldsymbol{\Delta}(j\omega)\big) \cdot \big(\boldsymbol{I} - \boldsymbol{\Delta}^*(j\omega)\big) &= \mathrm{diag}_N(2 - 2\cos(\delta_1\omega), \ldots \\ &\quad \ldots, 2 - 2\cos(\delta_N\omega)). \quad (37) \end{aligned}$$

Hence, the singular values of the operator $\big(\boldsymbol{I} - \boldsymbol{\Delta}(j\omega)\big)$ are $\{\sqrt{2 - 2\cos(\delta_i\omega)}\}_{i=1}^N$. Using

$$1 - \cos(x) \le |x|, \quad x \in \mathbb{R}, \tag{38}$$

that can be easily verified, we indeed prove (35).

To show (36), it is sufficient to note that $\boldsymbol{\Phi}(j\omega)$ is a diagonal operator with strictly proper rational functions in the diagonal. Its maximum singular values hence decay at least as fast as $\mathcal{O}(|\omega|^{-1})$ when $|\omega| > \overline{\omega}$, and are bounded when $|\omega| \le \overline{\omega}$, which in fact implies (36). ■

We use the result of Lemma 1 to derive the bound for the composite operator $\boldsymbol{\Phi} - \boldsymbol{\Phi}\boldsymbol{\Delta}$ based on $\overline{\delta}$.

Proposition 6: The following inequality holds:

$$\|\boldsymbol{\Phi} - \boldsymbol{\Phi}\boldsymbol{\Delta}\|_\infty \le \overline{C}\sqrt{\overline{\delta}}, \tag{39}$$

for some $\overline{C} > 0$.

Proof: Let $u = \boldsymbol{\Phi} f$ and $g = (\boldsymbol{I} - \boldsymbol{\Delta})u$, then $g = (\boldsymbol{\Phi} - \boldsymbol{\Delta}\boldsymbol{\Phi})f$. Hence:

$$\begin{aligned} \|\boldsymbol{G}(j\omega)\|_2 &= \|\big(\boldsymbol{I} - \boldsymbol{\Delta}(j\omega)\big)\boldsymbol{\Phi}(j\omega)F(j\omega)\|_2 \\ &\le \sigma_{\max}[\boldsymbol{I} - \boldsymbol{\Delta}(j\omega)] \cdot \sigma_{\max}[\boldsymbol{\Phi}(j\omega)] \cdot \|F(j\omega)\|_2. \end{aligned}$$

Using the result of Lemma 1 for $\omega > \overline{\omega}$ we derive

$$\begin{aligned} \int_{|\omega|>\overline{\omega}} \|\boldsymbol{G}(j\omega)\|_2^2 d\omega &\le \int_{|\omega|>\overline{\omega}} 2\overline{\delta}|\omega| \cdot \frac{C_\Phi^2}{|\omega|} \cdot \|F(j\omega)\|_2^2 d\omega \\ &\le 4\pi\overline{\delta}C_\Phi^2 \cdot \|f\|_2^2. \quad (40) \end{aligned}$$

Similarly, for $\omega \le \overline{\omega}$, we can obtain

$$\begin{aligned} \int_{|\omega|\le\overline{\omega}} \|\boldsymbol{G}(j\omega)\|_2^2 d\omega &\le \int_{|\omega|\le\overline{\omega}} 2\overline{\delta}|\omega| \cdot C_\Phi^2 \cdot \|F(j\omega)\|_2^2 d\omega \\ &\le 4\pi\overline{\delta}C_\Phi^2\overline{\omega} \cdot \|f\|_2^2. \quad (41) \end{aligned}$$

From (40) and (41) we can easily obtain

$$\|\boldsymbol{g}\|_2 \le \overline{C} \cdot \|f\|_2, \tag{42}$$

for

$$\overline{C} = 2C_\Phi\sqrt{(\overline{\omega} + 1)}. \tag{43}$$

Equation (42) indeed implies (39). ■

The following theorem shows the robustness of the induced error system $\mathcal{K}$ against the delay jitters $\{\delta_i\}_{i=1}^N$.

Theorem 2: In the presence of delay estimate errors, the induced error system $\mathcal{K}$ is robust in the sense that its $\mathcal{H}_\infty$ norm is bounded as

$$\|\mathcal{K}\|_\infty \le \|\mathcal{W} - \mathcal{F}\boldsymbol{\Phi}\|_\infty + \sqrt{\overline{\delta}} \cdot \overline{C} \cdot \|\mathcal{F}\|_\infty, \tag{44}$$

where $\overline{\delta}$ is the maximum jitters and C_Φ is defined as in (36).

Proof: Indeed:

$$\begin{aligned} \|\mathcal{K}\|_\infty &= \|\mathcal{W} - \mathcal{F}\boldsymbol{\Phi}\boldsymbol{\Delta}\|_\infty \\ &\le \|\mathcal{W} - \mathcal{F}\boldsymbol{\Phi}\|_\infty + \|\mathcal{F}\Phi - \mathcal{F}\boldsymbol{\Phi}\boldsymbol{\Delta}\|_\infty \\ &\le \|\mathcal{W} - \mathcal{F}\boldsymbol{\Phi}\|_\infty + \sqrt{\overline{\delta}} \cdot \overline{C} \cdot \|\mathcal{F}\|_\infty. \end{aligned}$$

■

A consequence of Theorem 2 is that the induced error system $\mathcal{K}$ is robust against the delay estimate errors $\{\delta_i\}_{i=1}^N$. In fact, its performance is degraded from the design performance $\|\mathcal{W} - \mathcal{F}\boldsymbol{\Phi}\|_\infty$, in the worst case, by an additional term of order $\mathcal{O}(\sqrt{\overline{\delta}})$.

VI. Experimental Results

We present in Section VI-A an example of FIR filter design. Experiments on IIR filter design can be found in our conference paper [23]. In Section VI-B, we compare the performance of the proposed method to existing methods.

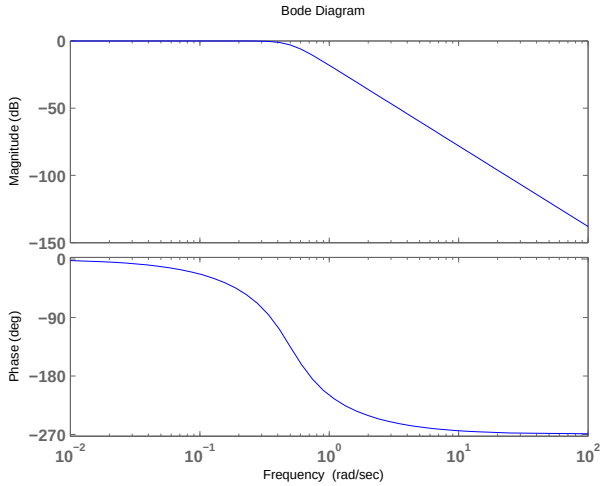

Fig. 9. The magnitude and phase response of the transfer function $\Phi(s)$ modeling the measurement devices. We use $\Phi_i(s) = \Phi(s)$ for $i = 0, 1, 2$.

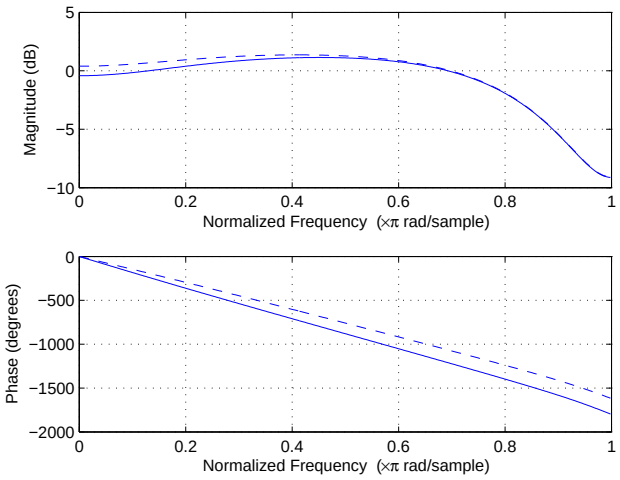

Fig. 11. The magnitude and phase response of synthesis FIR filters $F_1(z)$ (dashed), and $F_2(z)$ (solid) designed using the proposed method.

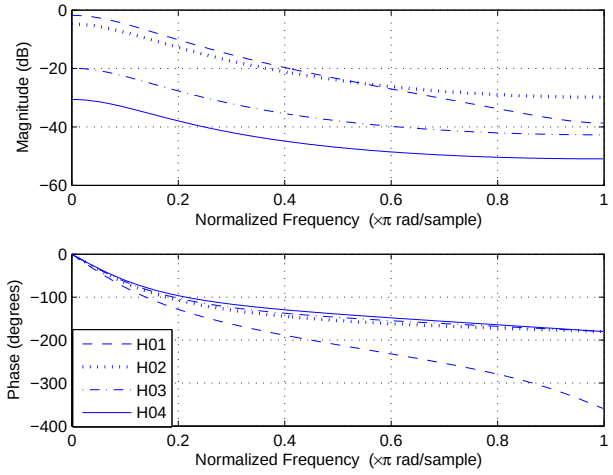

Fig. 10. The equivalent analysis filters $\boldsymbol{H}_0(z)$ of the first channel. Since $\boldsymbol{H}_0(z)$ takes multiple inputs, in this case $n_u = 4$ inputs, the i-th input is passed through filter $\boldsymbol{H}_{0i}(z)$ for $1 \le i \le 4$.

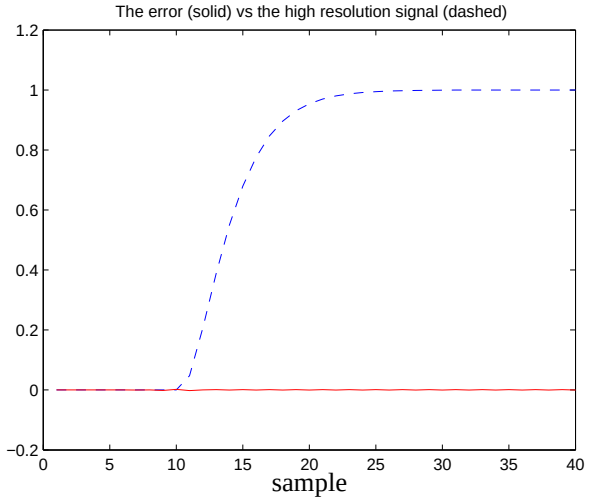

Fig. 12. The error $e[n]$ (solid) plotted against the desired output $y_0[n]$ (dashed). The $\mathcal{H}_\infty$ norm of the system is $\|\mathcal{K}\|_\infty \approx 4\%$.

A. Example of FIR filter design

The experimental setting is as follows:

- We use two channels to double the resolution; that is, $M = N = 2$.
- All functions $\Phi_i(s) = \omega_c^2/(s + \omega_c)^2$ for $\omega_c = 0.5$ and $i = 0, 1, 2$. Fig. 9 plots the Bode diagram of the transfer function $\Phi_i(s)$.
- Input signal is a step function:

$$f(t) = \begin{cases} 0 & t < 0.3 \\ 1 & t \ge 0.3. \end{cases} \tag{45}$$

- $m = 10, h = 1, D_1 = 1.2, D_2 = 0.6$.
- Maximum filter length is $nM = 22$.

In Fig. 10, we show the equivalent filters $\boldsymbol{H}_0(z)$ of the first channel. Note that $\boldsymbol{H}_i(z)$, for $i = 0, 1, 2$, take multiple inputs (in this case $n_u = 4$ inputs, hence 4 filters for each $\boldsymbol{H}_i(z)$ are required). The magnitude and phase response of the designed filters $F_1(z), F_2(z)$ are shown in Fig. 11. In Fig. 12, we show the error $e[n]$ of the induced system (solid) and the desired output $y_0[n]$ (dashed). The $\mathcal{H}_\infty$ norm of the system is $\|\mathcal{K}\|_\infty \approx 4\%$. Observe that the induced error $e[n]$ is small compared to the desired signal $y_0[n]$.

We also test the robustness of $\mathcal{K}$ against jitters $\{\delta_i\}_{i=1,2}$. The synthesis filters are designed for $\widehat{D}_1 = 1.2h$ and $\widehat{D}_2 = 0.6h$, but the system uses inputs produced with jittered time delays D_1, D_2. Figure 13 shows the $\mathcal{H}_\infty$ norm of the induced errors plotted against jitters in δ_1 (solid) and δ_2 (dashed). The errors are observed to be robust against delay estimate errors. Note that the intersection of two curves (where no jitter is present) is not necessary a local minima of either curves.

B. Comparison to existing methods

We compare the proposed method to an existing method, called the Sinc method. The Sinc method tested here approximates the fractional delay operator e^{-Ds} by an FIR filter using

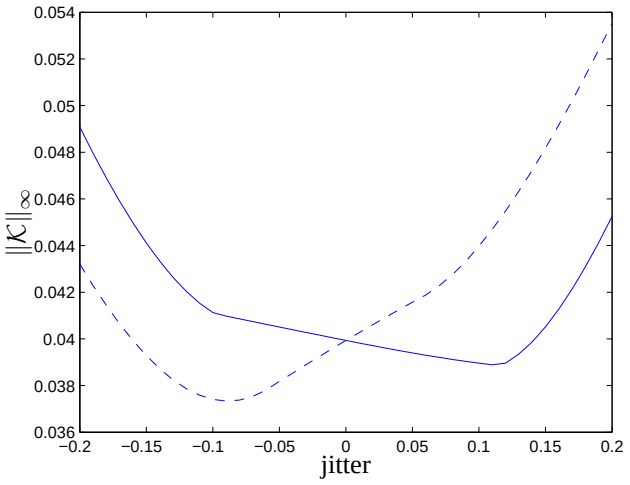

Fig. 13. The norm $\|\mathcal{K}\|_\infty$ of the induced error system plotted against jitters δ_1 (solid) and δ_2 (dashed). The system's robustness against jitters δ_1 and δ_2 is guaranteed by Theorem 2.

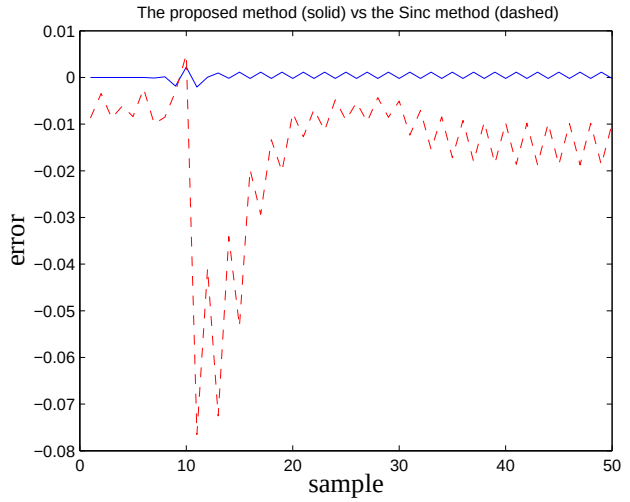

Fig. 14. Performance comparison of the error of the proposed method (solid) and of the Sinc method truncated to 23 taps (dotted).

the function $\mathrm{sinc}(x) = \sin(\pi x)/(\pi x)$:

$$F_D^{(sinc)}[n] = \mathrm{sinc}\Big(n - \frac{D}{2h}\Big),$$

with $|n| \leq N_{cutoff} = 11$. Hence tested filters of the Sinc method are of 23 taps. Note that, in the formula above, the sampling interval is $2h$.

The Sinc method filters the low resolution signal $x_1[n]$ by the approximated FIR filter $F_{D_1}^{(sinc)}$ to get the *even* samples of $y_0[n]$, and filters the second low resolution signal $x_2[n]$ by the approximated FIR filter $F_{D_2+h}^{(sinc)}$ to get the *odd* samples of $y_0[n]$. In other words, the high resolution signal is obtained by interleaving individually filtered low resolution channels.

Figure 14 compares the error of the proposed method to the error of the Sinc method. Both sets of synthesis filters have similar length (length 23 for the Sinc method and length 22 for the proposed method). We observe that the proposed method shows a better performance, especially around the discontinuity.

TABLE I

PERFORMANCE COMPARISON IN ROOT MEAN SQUARE ERROR (RMSE), MAXIMUM ERROR (MAX), AND STEADY-STATE ERROR (SS). THE LENGTH OF SYNTHESIS FILTERS ARE 23 FOR THE SINC METHOD AND 22 FOR THE SEPARATION AND PROPOSED METHOD. FIRST THREE COLUMNS USE THE STEP FUNCTION IN (45) AS INPUT. THE LAST TWO COLUMNS USE INPUT $f(t) = \cos(0.3t) + \cos(0.8t)$.

	RMSE_1	Max_1	SS	RMSE_2	Max_2
Sinc	0.0171	0.0765	-0.0143	0.0689	0.1777
Separation	0.0029	0.0293	0.0018	0.0092	0.0506
Proposed	0.0008	0.0023	0.0006	0.0019	0.0079

The improved performance of the proposed technique in Fig. 14 is due to two reasons. First, replacing fractional delays $\{e^{-D_i s}\}_{i=1}^N$ by equivalent analysis filters $\{\boldsymbol{H}_i(z)\}_{i=1}^N$ enhances the results. Second, the use of $\mathcal{H}_\infty$ optimization allows the system to perform even for inputs that are not necessarily bandlimited.

We also compare the proposed method to a second method, called the Separation method. This method, similar to the Sinc method above, obtains the high resolution signal by interleaving individually processed low resolution channels. What distinguishes the Separation method from the Sinc method is that the Separation method approximates the fractional delay operator e^{-Ds} by an FIR operator designed to minimize the $\mathcal{H}_\infty$ norm of an induced error system [22].

Figure 15 compares the error of the proposed method and the Separation method, all synthesis filters are of length 22. Again, the proposed method hence yields a better performance. This is expected as the synthesis filters are designed together, allowing effective joint processing of all low resolution signals.

Table I shows the comparison of the three methods for two inputs of different characteristics: a step function as in (45) and a bandlimited function $f(t) = \cos(0.3t)+\cos(0.8t)$. Synthesis filters of 23 taps are used for the Sinc method and of 22 taps are used for the Separation and proposed methods. The errors are compared in terms of the root mean square error (RMSE), the maximum value (Max), and the average value in steady-state regime (SS) when the step function in (45) is used as input. As observed in Fig. 14 and Fig. 15, in the steady-state regime, the system errors are periodic (with period 2). Hence the errors alternate between two values; the steady-state error in Table I is computed as the average of these two values. As can be seen, the proposed method consistently outperforms existing methods.

Another method worth mentioning is the method proposed by Shu et al. [26], in which digital synthesis filters are designed to minimize the $\mathcal{H}_\infty$ norm of a hybrid filter bank with rational analysis filters. Both the method proposed by Shu et al. and ours convert a hybrid system to a digital system and using $\mathcal{H}_\infty$ optimization to design the synthesis filters. However, Shu el al. consider only rational analysis filters whereas we consider fractional delays. Hence, Table I also offers an indirect comparison of both methods, where fractional delay operators are approximated as in the Sinc and Separation methods.

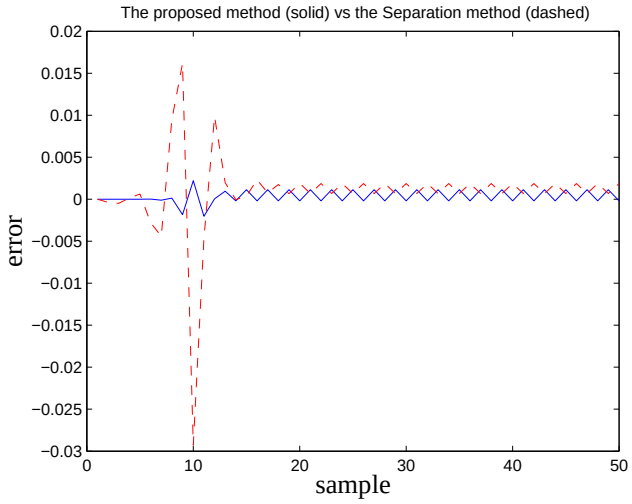

Fig. 15. Error comparison between the proposed method (solid) and the Separation method (dotted).

VII. Conclusion and Discussion

In this paper, we designed digital synthesis filters for a hybrid multirate filter bank with fractional delays, with potential applications in multichannel sampling. We showed that this hybrid system is $\mathcal{H}_\infty$-norm equivalent to a digital system. The equivalent digital system then can be used to design stable synthesis filters, using model-matching or linear matrix inequality methods. We also showed the robustness of the induced error system in the presence of delay estimate errors. Experimental results confirmed the superior performance of the proposed method compared to existing methods.

A limitation of the proposed method is the lack of an explicit solution for the system $\boldsymbol{F}(z)$ or the synthesis filter $\{F_i(z)\}_{i=1}^N$. This drawback can be compensated with the wide availability of design implementations. Moreover, the design is performed only once for all input signals.

For future work, we would like to investigate the relationship between the upsampling rate M and the number of low resolution channels N to guarantee a predefined performance. Another direction is to design synthesis filters taking into account the uncertainties in the first place, using traditional robust control techniques [7].

MATLAB code for filter design procedures and experiments in this paper can be downloaded from the MATLAB Central (www.mathworks.com/matlabcentral).

Appendix
Computation of the norm of $\boldsymbol{B}\boldsymbol{B}^*$

We present how to compute the norm of the product $\boldsymbol{B}\boldsymbol{B}^*$. The adjoint operators of $\{\boldsymbol{Q}_i\}_{i=0}^N$ and $\{\boldsymbol{R}_i\}_{i=1}^N$ are:

$$(\boldsymbol{Q}_i^* x)(t) = B_i^T e^{(h-t)A_i^T} x \quad (46)$$

$$(\boldsymbol{R}_i^* x)(t) = \mathbf{1}_{[0,h-d_i)} B_i^T e^{(h-d_i-t)A_i^T} C_i^T x. \quad (47)$$

Hence, the adjoint operator of $\boldsymbol{B}_i$ is $\boldsymbol{B}_i^* = [\boldsymbol{Q}_i^*, \boldsymbol{R}_i^*]$ and the adjoint operator of $\boldsymbol{B}$ is $\boldsymbol{B}^* = [\boldsymbol{Q}_0^*, \boldsymbol{B}_1^*, \ldots, \boldsymbol{B}_N^*]$. Lemma 2 provides a formula to compute the product $\boldsymbol{B}\boldsymbol{B}^*$.

Lemma 2: The operator $\boldsymbol{B}\boldsymbol{B}^*$ is a linear operator characterized by a symmetric matrix $\Delta = (\Delta_{ij})_{i,j=0}^N$ with:

$$\Delta_{ij} = \begin{cases} \boldsymbol{Q}_0\boldsymbol{Q}_0^*, & \text{if } i=j=0 \\ \boldsymbol{Q}_0\boldsymbol{B}_j^* = \begin{bmatrix} \boldsymbol{Q}_0\boldsymbol{Q}_j^* & \boldsymbol{Q}_0\boldsymbol{R}_j^* \end{bmatrix}, & \text{if } 0=i<j \\ \boldsymbol{B}_i\boldsymbol{B}_j^* = \begin{bmatrix} \boldsymbol{Q}_i\boldsymbol{Q}_j^* & \boldsymbol{Q}_i\boldsymbol{R}_j^* \\ \boldsymbol{R}_i\boldsymbol{Q}_j^* & \boldsymbol{R}_i\boldsymbol{R}_j^* \end{bmatrix}, & \text{if } 0<i\le j \\ \Delta_{ji}^T, & \text{if } i>j. \end{cases}$$

Each block Δ_{ij} is composed by components of forms $\boldsymbol{Q}_i\boldsymbol{Q}_j^*, \boldsymbol{Q}_i\boldsymbol{R}_j^*$ and $\boldsymbol{R}_i\boldsymbol{R}_j^*$ that can be computed as:

$$\boldsymbol{Q}_i\boldsymbol{Q}_j^* = \boldsymbol{M}_{ij}(h) \quad (48)$$

$$\boldsymbol{Q}_i\boldsymbol{R}_j^* = e^{d_jA_j}\boldsymbol{M}_{ij}(h-d_j)C_j^T \quad (49)$$

$$\boldsymbol{R}_i\boldsymbol{R}_j^* = \begin{cases} C_i e^{(d_j-d_i)A_i}\boldsymbol{M}_{ij}(h-d_j)C_j^T, & \text{if } d_i<d_j \\ C_i\boldsymbol{M}_{ij}(h-d_i)e^{(d_i-d_j)A_i^T}C_j^T, & \text{if } d_i\ge d_j, \end{cases} \quad (50)$$

where

$$\boldsymbol{M}_{ij}(t) := \int_0^t e^{\tau A_i} B_i B_j^T e^{\tau A_j^T} d\tau. \quad (51)$$

Proof: We show here the proof of (50), the proof of (48) and (49) are similar. Consider the case $d_i < d_j$. For any x of appropriate dimension we have:

$$\begin{aligned} \left(\boldsymbol{R}_i\boldsymbol{R}_j^*\right)x &= C_i\int_0^{h-d_i} e^{(h-d_i-\tau)A_i}B_i(\boldsymbol{R}_j^*x)(\tau)d\tau \\ &= \left(C_i e^{(d_j-d_i)A_i}\boldsymbol{M}_{ij}(h-d_j)C_j^T\right)x. \end{aligned}$$

Hence if $d_i < d_j$ we indeed verify:

$$\boldsymbol{R}_i\boldsymbol{R}_j^* = C_i e^{(d_j-d_i)A_i}\boldsymbol{M}_{ij}(h-d_j)C_j^T.$$

The proof is similar for the case where $d_i \ge d_j$. ■

Finally, note that $\boldsymbol{M}_{ij}(t)$ can be efficiently computed as [19]:

$$\boldsymbol{M}_{ij}(t) = e^{A_it}\pi_{12}(t),$$

where $\pi_{12}(t)$ is the block $(1,2)$ of the matrix:

$$\begin{bmatrix} \pi_{11}(t) & \pi_{12}(t) \\ 0 & \pi_{22}(t) \end{bmatrix} = \exp\left(\begin{bmatrix} -A_i & B_iB_j^T \\ 0 & A_j^T \end{bmatrix} t\right).$$

References

[1] V. Balakrishnan and L. Vandenberghe, "Linear matrix inequalities for signal processing: An overview," in *Proceedings of the 32nd Annual Conference on Information Sciences and Systems*, Princeton, NJ, March 1998.

[2] J. Benesty, J. Chen, and Y. Huang, "Time-delay estimation via linear interpoation and cross correlation," *IEEE Trans. Speech Audio Proc.*, vol. 12, no. 5, pp. 509–519, September 2004.

[3] S. Boyd, L. El Ghaoui, E. Feron, and V. Balakrishnan, *Linear Matrix Inequalities in System and Control Theory*, ser. Studies in Applied Mathematics. Philadelphia, PA: SIAM Journ. of Math. Anal., 1994.

[4] T. Chen and B. Francis, "Design of multirate filter banks by $\mathcal{H}_\infty$ optimization," *IEEE Trans. Signal Proc.*, vol. 43, no. 12, pp. 2822–2830, December 1995.

[5] ——, *Optimal Sampled-Data Control Systems*. London, U.K.: Springer, 1995.

[6] R. Y. Chiang and M. G. Safonov, "MATLAB - robust control toolbox," http://www.mathworks.com, 2005.

[7] G. E. Dullerud and F. Paganini, *A Course in Robust Control Theory: A Convex Approach*. New York, NY: Springer-Verlag, 2000.

[8] J. Franca, A. Petraglia, and S. K. Mitra, "Multirate analog-digital systems for signal processing and conversion," in *Proc. IEEE*, vol. 35, no. 2, February 1997, pp. 242–262.

[9] B. Francis, *A Course in $\mathcal{H}_\infty$ Control Theory*. Heidelberg, Germany: Springer-Verlag, 1987.

[10] P. Gahinet and P. Apkarian, "A linear matrix inequality approach to $\mathcal{H}_\infty$ control," *International Journal of Robust and Nonlinear Control*, vol. 4, pp. 421–448, 1994.

[11] P. Gahinet, A. Nemirovski, A. J. Laub, and M. Chilali, "LMI control toolbox," http://www.mathworks.com, 1995.

[12] M. Green and D. J. N. Limebeer, *Linear Robust Control*. Upper Saddle River, NJ: Prentice-Hall, Inc., 1995.

[13] C. Herley and P. W. Wong, "Minimum rate sampling and reconstruction of signals with arbitrary frequency support," *IEEE Trans. Info. Theory*, vol. 45, no. 5, pp. 1555–1564, July 1999.

[14] O. S. Jahromi and P. Aarabi, "Theory and design of multirate sensor arrays," *IEEE Trans. Signal Proc.*, vol. 53, no. 5, May 2005.

[15] C. H. Knapp and G. C. Carter, "The generalized correlation method for estimation of time delay," *IEEE Trans. Acoust., Speech, and Signal Proc.*, vol. ASSP-24, no. 4, pp. 320–327, August 1976.

[16] T. I. Laakso, V. Valimaki, M. Karjalainen, and U. K. Laine, "Splitting the unit delay - tools for fractional delay filter design," *IEEE Signal Proc. Mag.*, vol. 13, no. 1, pp. 30–60, 1996.

[17] J. Lam, "Model reduction of delay systems using Pade approximation," *International Journal of Control*, vol. 57, no. 2, pp. 377–391, February 1993.

[18] B. P. Lathi, *Linear Systems and Signals*, 2nd ed. New York, NY: Oxford University Press, 1992.

[19] C. F. V. Loan, "Computing integrals involving the matrix exponential," *IEEE Trans. Autom. Control*, vol. 23, no. 3, pp. 395–404, June 1978.

[20] P. Marziliano and M. Vetterli, "Reconstruction of irregularly sampled discrete-time bandlimited signals with unknown sampling locations," *IEEE Trans. Signal Proc.*, vol. 48, no. 12, pp. 3462–3471, December 2000.

[21] M. Nagahara and Y. Yamamoto, "Optimal design of fractional delay filters," *IEEE Conference on Decision and Control*, vol. 6, pp. 6539–6544, December 2003.

[22] ——, "Optimal design of fractional delay FIR filters without band-limiting assumption," *Proc. IEEE Int. Conf. Acoust., Speech, and Signal Proc.*, vol. 4, pp. 221–224, March 2005.

[23] H. T. Nguyen and M. N. Do, "Signal reconstruction from a periodic nonuniform set of samples using $\mathcal{H}_\infty$ optimization," in *Proc. of SPIE*, vol. 6498, San Jose, February 2007.

[24] L. D. Philipp, A. Mahmood, and B. L. Philipp, "An improved refinable rational approximation to the ideal time delay," *IEEE Trans. Circ. and Syst.*, vol. 46, no. 5, pp. 637–640, May 1999.

[25] R. G. Shenoy, D. Burnside, and T. W. Parks, "Linear periodic systems and multirate filter design," *IEEE Trans. Signal Proc.*, vol. 42, no. 9, pp. 2242–2256, September 1994.

[26] H. Shu, T. Chen, and B. Francis, "Minimax design of hybrid multirate filter banks," *IEEE Trans. Circ. and Syst.*, vol. 44, no. 2, February 1997.

[27] D. Slepian, "On bandwidth," in *Proc. IEEE*, vol. 64, no. 3, 1976, pp. 292–300.

[28] P. P. Vaidyanathan, *Multirate Systems and Filter Banks*. New York, NY: Prentice Hall, 1993.

[29] M. Vetterli and J. Kovačević, *Wavelets and Subband Coding*. New York, NY: Prentice-Hall, 1995.

[30] F. Viola and W. F. Walker, "A spline-based algorithm for continuous time-delay estimation using sampled data," *IEEE Trans. Ultrasonics, Ferroelectrics, and Frequency Control*, vol. 52, no. 1, pp. 80–93, January 2005.

[31] Y. Yamamoto, B. D. O. Anderson, M. Nagahara, and Y. Koyanagi, "Optimal FIR approximation for discrete-time IIR filters," *IEEE Signal Proc. Letters*, vol. 10, no. 9, pp. 273–276, September 2003.

[32] M. G. Yoon and B. H. Lee, "A new approximation method for time-delay systems," *IEEE Trans. Autom. Control*, vol. 42, no. 7, pp. 1008–1012, July 1997.